

“Mitonuclear genetics of neurodegeneration in Drosophila models of Alzheimer’s disease”

Mitochondrial dysfunction is a shared condition among the major neurodegenerative disorders, including Alzheimer’s disease and related dementias (AD/ADRD), Parkinson’s disease and amyotrophic lateral sclerosis (ALS). The high energy demands of the brain and other neural tissues require constant mitochondrial activity to maintain normal function. Mitochondrial function requires the coordinated expression of 37 genes encoded in mitochondrial DNA (mtDNA) inside mitochondria and over 1000 nuclear-encoded genes whose products must be transported into mitochondria. Defects in communication between these two genomes can reduce ATP production and alter cellular redox state, calcium signaling, organelle fission and fusion essential for cellular and organismal health. This proposal will use the power of Drosophila genetic models to dissect ‘mitonuclear communication’ at the genetic, cellular and molecular levels, *in vivo*. We combine the distinct expertise of two laboratories that have developed complementary approaches to dissecting mitochondrial dysfunction. The Rand lab has introduced genetically distinct mtDNAs into controlled nuclear genetic backgrounds to disrupt mitonuclear communication altering OXPHOS, ROS levels, nuclear gene expression and aging. The Wharton lab has developed knock-in mutant models of the genes causing ALS-FTD that have identified novel defects in neural circuitry and synaptic mitochondrial morphology. They have further identified genes in carbohydrate and nucleic acid metabolism pathways (pentose phosphate, purine and NAD) that suppress these disease states by altering mitochondrial morphology, motor function, and lifespan. The long term goal of this research program is to use the Drosophila genetic model to identify the joint mitochondrial- and nuclear-genomic factors responsible for communication defects in neurodegenerative diseases. The objectives of this proposal are to identify the mechanisms of mitochondrial and metabolic defects underlying ADRD phenotypes caused by epistatic interactions between mutations in the nuclear genes SOD, A- β and Tau when paired with specific mtDNAs that disrupt mitochondrial biogenesis. Our working hypothesis is that mitochondrial-nuclear epistatic interactions modify metabolite profiles (e.g., ATP, NAD⁺/NADH, ROS) underlying cellular communication essential for mitochondrial health. **Aim 1 will identify the individual and epistatic effects of altered mitonuclear genome pairs mutant models of ADRD (e.g., SOD1, A- β , tau).** **Aim 1A** will identify the mitonuclear communication pathways in ADRD models. **Aim 1B** will validate the mechanisms of action using tissue specific overexpression and knockdown of pathway members. **Aim 2 will determine the impact of altered mitonuclear communication on alleviation of neurodegeneration by known genetic suppressors.** **Aim 2A** will identify the modifications to mitonuclear pathways that are responsible for the suppression of ADRD. **Aim 2B** will determine the degenerative nature of the ADRD phenotypes through time course analyses of mutant and genetically suppressed mitonuclear ADRD genotypes.

Mitochondrial dysfunction is a shared cellular phenotype and driver of neurotoxicity among the major neurodegenerative disorders (ND), such as Alzheimer's disease and related dementias (AD/ADRD), amyotrophic lateral sclerosis (ALS)/frontotemporal dementia (FTD), and Parkinson's disease. The high energy demands of the brain and other neural tissues require constant mitochondrial activity to maintain normal function, but the biology of mitochondria makes this challenge tremendously complex. Mitochondrial function requires the coordinated expression of 37 genes encoded in mitochondrial DNA (mtDNA) inside mitochondria, and over 1000 nuclear-encoded genes whose products must be transported into mitochondria. ATP production by oxidative phosphorylation (OXPHOS) is the primary product of this dual genome communication. Mitochondrial homeostasis is impacted by multiple mechanisms, such as the cellular redox state, balanced calcium signaling, trafficking/axonal transport, fission-fusion dynamics, and mitophagy. Importantly, each process has been implicated as a causal factor in ADRD. The complex dynamics between these two genomes are important barriers to understanding the etiology of ADRD diseases and hinder the development of treatments. The research proposed here, pairing specific mtDNA mutations with known nuclear ADRD models, provides expertise that will identify factors essential for optimal mitonuclear communication.

The Rand lab has developed *Drosophila* genetic models that provide a powerful functional approach to molecularly dissect the complexity of mitonuclear communication at the cellular level in an *in vivo* context. We have disrupted mitonuclear communication by introducing genetically distinct mtDNAs into controlled nuclear genetic backgrounds altering OXPHOS, ROS levels, nuclear gene expression, and aging. We have mapped mitonuclear interactions to individual nucleotides in each genome that cause OXPHOS defects related to human exercise intolerance. The Wharton lab has characterized morphological and functional defects in mitochondria associated with genetic models of ALS/FTD that harbor knock-in mutations identical to those found in patients. Our models exhibit defects in neural circuitry, synaptic morphology and function, in addition to early changes in the abundance, networking and survival of mitochondria in different subcellular compartments of neurons. We have identified multiple genetic suppressors of these mitochondrial defects, as well as neurodegenerative phenotypes that include loss in synaptic integrity, reduced locomotor function and lifespan. These suppressor genes act in the OXPHOS, carbohydrate and nucleotide biosynthesis pathways (purine and NAD) altering metabolomic and transcriptomic profiles of the ALS/FTD models. These models provide a powerful set of molecules and pathways to probe mitonuclear communication in an *in vivo* ADRD context. The long term goal of this research program is to use the *Drosophila* model to identify the joint mitochondrial- and nuclear-genomic factors responsible for the breakdown of proper mitonuclear communication that leads to neurodegenerative diseases. The objectives of this proposal are to identify the mechanisms of mitochondrial and metabolic defects underlying degenerative phenotypes caused by epistatic interactions between specific mtDNAs and three nuclear ADRD models (SOD1, A β , and Tau). Our working hypothesis is that mitonuclear epistatic interactions modify metabolite profiles (e.g., ATP, NAD⁺/NADH, ROS) essential for mitochondrial health in the progression of ADRD.

Aim 1. Identify factors underlying ADRD neurodegeneration in disrupted mitonuclear genome pairs.

We will identify (**Aim 1A**) and validate (**Aim 1B**) genes and metabolites critical for mitonuclear communication that underlie the defects associated with ADRD by quantifying altered neurodegenerative phenotypes, mitochondrial bioenergetics and gene expression in disrupted and intact mtDNA-nuclear gene pairs. Validation in **Aim 1B** will be accomplished by gene and tissue-specific manipulation in disrupted and intact mitonuclear genetic combinations.

Aim 2. Identify factors underlying suppression of ADRD neurodegeneration in disrupted mitonuclear genome pairs. **Aim 2A.** We will identify key mitonuclear communication factors that alleviate the progression of ADRD by comparing disrupted and intact mitonuclear genotypes in the context of suppressed degeneration. **Aim 2B.** Define the mechanistic basis underlying the suppression of ADRD phenotypes through manipulation of metabolite profiles of mutant and genetically suppressed ADRD genotypes in disrupted and intact mitonuclear combinations.

The expected outcomes of these Aims are the identification of the mitonuclear genetic basis underlying biochemical networks governing the degenerative nature of ADRD. Our findings will accelerate the development of mammalian models of mitonuclear communication in ADRD and can lead to more efficient analyses of precious patient samples in the search for effective therapies.

1. Significance

Alzheimer's disease (AD) is a progressive neurodegenerative condition of the brain that is the 5th leading cause of death among people over 65¹. Treatments for AD are lacking due to the complex and cryptic causes that begin years before symptoms and vary among patients. Despite years of research, much of it focused on amyloid plaques containing A β and intracellular neurofibrillary tangles of tau protein, there is limited understanding of the mechanisms underlying degeneration of individual neurons, brain function and mortality.

A wealth of data has identified associations between AD and declining mitochondrial activity^{2,3} including links between A β and mitochondrial decline^{4,5}. Mitochondrial dysfunction is a shared cellular phenotype and driver of neurotoxicity among the major neurodegenerative disorders (ND), such as Alzheimer's disease and related dementias (AD/ADRD), amyotrophic lateral sclerosis (ALS)/frontotemporal dementia (FTD), and Parkinson's disease. The brain is 2% of the human body weight, but it consumes 20% of the body's ATP. The high energy demands of the brain and other neural tissues require constant mitochondrial activity to maintain normal function. The role of mitochondrial dysfunction in ADRDs has two sources of complexity that impede research progress. The brain has ~100 billion neurons, a similar number of glial cells and >100 trillion synapses. In addition, mitochondrial function requires the coordinated expression of 37 genes encoded in mitochondrial DNA (mtDNA) inside mitochondria, and over 1200 nuclear-encoded genes whose products must be transported into mitochondria. ATP production by oxidative phosphorylation (OXPHOS) is the primary product of this dual genome communication, but mitochondrial homeostasis is impacted by multiple mechanisms, such as the cellular redox state, balanced calcium signaling, trafficking/axonal transport, fission-fusion dynamics, and mitophagy. Importantly, each process has been implicated as a causal factor in ADRD. The combined neuronal complexity of the brain and the communication between two genomes that power these neurons are critical barriers to discovering treatments for ADRD.

The research proposed here seeks to address this complexity by approaching the problem using an explicit dual, 'mitonuclear' genomic approach. By experimentally pairing distinct mtDNA genotypes with known nuclear models of ADRDs we can manipulate the bidirectional aspects of mitonuclear communication that contribute to ADRD progression. The objectives of this proposal are to identify the mechanisms of mitochondrial and metabolic defects underlying degenerative phenotypes caused by epistatic interactions between specific mtDNAs and three nuclear ADRD models (SOD1, A β , and Tau). Our working hypothesis is that mitonuclear epistatic interactions modify metabolite profiles (e.g., ATP, NAD⁺/NADH, ROS) that act as signaling molecules in mitonuclear communication. Disruption of this communication is a causal factor in ADRD. The complementary expertise of two established *Drosophila* geneticists, one focusing on mitochondrial genetics, and one focusing on neurodegenerative disease provides the expertise that can uniquely address the problem of mitonuclear communication in ADRD. Below we provide preliminary evidence in support of these goals and hypothesis.

Mitonuclear genetics in *Drosophila*

We have developed mitonuclear genetic models in *Drosophila* where a variety of different mtDNAs are introduced into distinct nuclear genetic backgrounds to disrupt normal mitonuclear communication and function. The logic behind these models is that 'native' or 'intact' mtDNA-nucDNA combinations (e.g., *D. melanogaster* mtDNA from the *D. melanogaster* OreR strain paired with the OreR nuclear genome) will have normal mitochondrial function, and 'foreign' or 'disrupted' mitonuclear pairings (e.g., mtDNAs from other species of *Drosophila* such as *D. simulans* or *D. yakuba* placed on a *D. melanogaster* OreR background) will have altered mitochondrial function. These models further predict that the degree of disruption will scale with the nucleotide and amino acid divergence between the native and foreign mtDNA sequences (Fig 1).

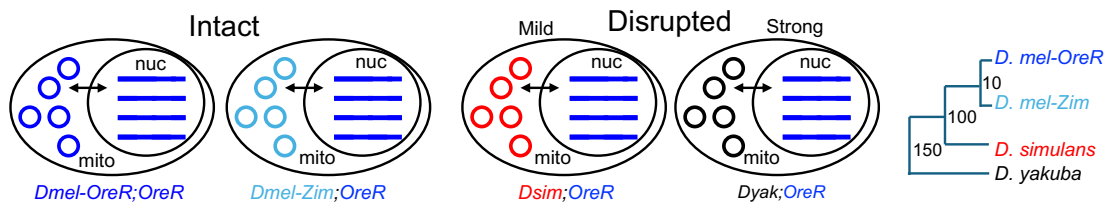


Fig 1. Native and disrupted mitonuclear pairings. Genotype notation = *mtDNA*; *nucDNA*. mtDNAs from the same species provide native or mild disruptions, while mtDNA from different species provide stronger disruption due to the larger number of amino acid changes that have accumulated during evolutionary divergence.

We have used these models to dissect the mitonuclear genetics of aging⁶, fitness⁷, mitochondrial translation and OXPHOS⁸, diet and caloric restriction⁹, mitochondrial respiration, oxidative stress and metabolomics¹⁰, epistasis and gene-environment interactions¹¹, exercise and climbing performance^{12,13}, altered nuclear gene expression under hypoxia¹⁴, TOR signaling via rapamycin¹⁵, glucose-protein diets¹⁶ and in distinct tissues¹⁷. Below we highlight a subset of these experiments to demonstrate the highly repeatable nature of these manipulations. Importantly, each mitonuclear pairing has distinct impacts on molecular, biochemical or organismal phenotypes, but the ‘strong disruptions’ using different species mtDNAs are viable and fertile and do not represent highly compromised genetic stocks.

Intact and disrupted mitonuclear genotypes were constructed with *D. melanogaster* OreR nuclear genomes paired with OreR mtDNA, a related Zim mtDNA, or with mtDNAs from *D. simulans* (sm21, Dmau, sm22, sm38). The disrupted pairings show reduced longevity compared to intact (Fig 2A). Interestingly, on a restricted 2% yeast diet, all strains showed longevity extension, but the disrupted *D. simulans* mtDNAs did not realize the same extension as the intact OreR;OreR mitonuclear genotype (Fig 2B). Notably the lifespans of all strains were indistinguishable on starvation and richer diets. This demonstrates that genes encoded in mtDNA are in the diet restriction pathway and that disrupted mitonuclear genotypes alter this response

We also found native mitonuclear genotypes (OreR, Zim on the OreR nuclear background) show enhanced mitochondrial O₂ consumption when exposed to rapamycin but disrupted mitonuclear genotypes (sm21, sil) eliminate this benefit (Fig 3A). Rapamycin clearly alters the carbohydrate profile of the native mitonuclear genotype (OreR) compared to control diet (blue vs. black polygons), but the disrupted mitonuclear genotype (sm21) has a carbohydrate profile that is unaffected by rapamycin treatment (Fig 3B). Nucleotide and NAD metabolites (Fig 3C) show similar results to those shown in Fig 3B. Glucose, phosphate, and nicotinamide riboside each exhibit different levels in the intact OreR;OreR genotype on control diet but levels are significantly different on rapamycin diet (Fig. 3D). The disrupted genotype sm21;OreR on control food has metabolite levels that are the same as the intact OreR;OreR on rapamycin, and it is insensitive to rapamycin¹⁸. These results demonstrate that altered mitonuclear communication induced by different mtDNAs mirror the effects of the TOR inhibitor rapamycin. Notably, the metabolic pathways affected in this mitonuclear model (glucose, purine and OXPHOS metabolism) overlap with pathways implicated in ADRD, establishing that this genetic model addresses the specific mitochondrial-nuclear communication goals of this RFA.

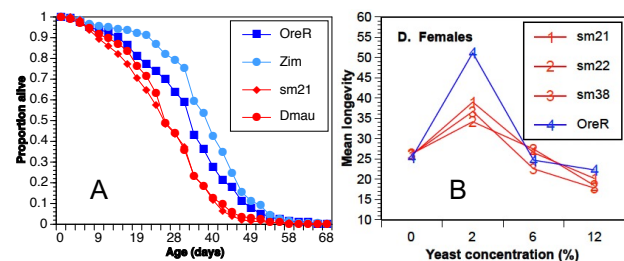


Fig. 2. Foreign mtDNAs compromise longevity and its extension by diet restriction. A. Longevity of alternative mitochondrial genotypes. B. Longevity of mitochondrial genotypes under diet restriction

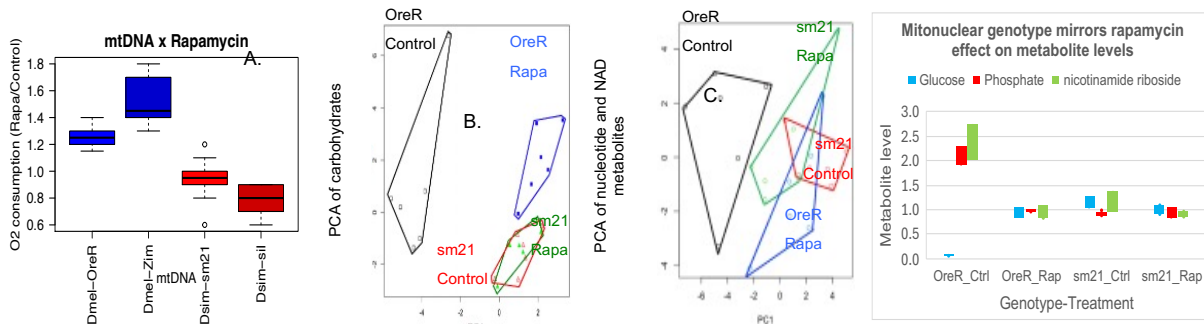


Fig. 3. Disrupted mitonuclear genotypes abrogate beneficial effects of rapamycin on mitochondrial respiration and mimic rapamycin's effect on metabolite profiles. A. O₂ consumption for different mitonuclear genotypes. B. PCA plots for carbohydrates (B) and nucleotides and NAD metabolites (C). D. Normalized values for three metabolites in glycolysis, OXPHOS and NAD metabolism.

We have also shown that mitochondrial genotypes can alter the transcriptional profile of nuclear genes. Four mitonuclear genotypes were exposed to a time course of hypoxia (6% O₂ for 0, 30, 120 minutes). These consisted of two intact: OreR mtDNA on two different *D. melanogaster* nuclear genomes (OreR;OreR and OreR;Austria-AutW132); and two disrupted: *D.simulans*-sil on the same two *D. melanogaster* nuclear genomes (sil;OreR and sil;AutW132). Each mitonuclear genotype has a distinct nuclear transcriptional profile in response to hypoxia (Fig 4A), but KEGG analyses show strong signals for mitochondrial dysfunction and hypoxia (Fig 4B). This establishes that alternative mtDNAs can act as trans-mediated modifiers of nuclear transcriptional modifiers. Because no gene products are exported from the mitochondria to the sites of nuclear transcription, this effect must be mediated by metabolites and other molecules that are a consequence of the altered metabolic state of the mitochondria with different mtDNAs^{3,5,19}. Related work on mitochondrial signaling in *C. elegans* neurons has identified serotonin, the neuropeptides FLP-1 and FLP-2, and the Wnt ligand, EGL-20 as 'mitokines'²⁰.

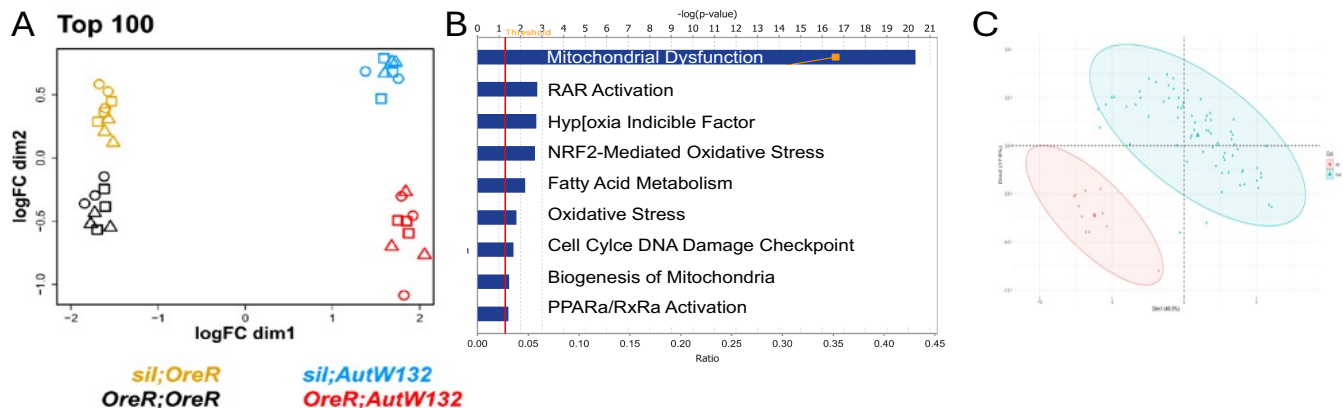


Fig. 4. Mitochondrial genotypes alter nuclear transcriptional responses to hypoxia and nutrients. A. Transcriptional profiles of nuclear genome is distinct for each mitonuclear pairing. B. Kegg pathway analysis. C. mtDNA (red) and nuclear (blue) encoded OXPHOS gene expression affected differently in *Sod1*^{A4V} mutants

Bulk RNAseq was performed in the Wharton lab on heads of dSod1^{WT}("silent") and dSod1^{A4V} mutants and among the differentially expressed genes (DEGs), GO term annotations for individual OXPHOS complexes identified both mtDNA- and nuclear-encoded genes. The direction and magnitude of the different gene sets were not highly concordant, with mtDNA genes down regulated in A4V mutants while WT are not (Fig 5). These data demonstrate that a Sod1 mutation associated with neurodegenerative disease can alter transcriptional profiles of both mtDNA-encoded and nuclear-encoded OXPHOS subunits but the direction of change is different suggesting a disconnect in communication between the mitochondrial and nuclear genomes.

Drosophila models of neurodegeneration

We will use multiple ADRD models to probe the sensitivity of these disease states to mitonuclear communication. Previous work in the Wharton lab has focused on multiple models ALS/FTD and given the overlap in cellular processes disrupted in ALS/FTD and AD, as well as the progression in

degeneration and presentation of cognitive decline, we will apply our knowledge and expertise to investigate the mechanisms underlying mitonuclear communication critical for neuronal health. The three *Drosophila* models of ADRD we will make use of are: knock-in mutations in the *Sod1* locus and two overexpression models the human A β 42 peptide²¹, and human *tau* harboring the R406W patient allele²². Here, we summarize data from the Wharton lab that sets the stage for our phenotypic assays and introduces a group of genetic suppressors which will aid in dissecting the pathway and factors responsible for maintaining mitonuclear communication in healthy neurons.

We have generated two knock-in mutations of the most common patient alleles in North America, SOD1^{G85R} and SOD1^{A4V} (hereafter, G85R and A4V)²³ in the endogenous *Drosophila Sod1* gene^{24,25}. Dysregulation of superoxide dismutase 1 (SOD1) is associated with amyotrophic lateral sclerosis/frontotemporal dementia (ALS/FTD) and Alzheimer's disease (AD)^{3,5}. SOD1 is critical for catalyzing the removal of superoxide free radicals regulating reactive oxygen species (ROS) produced as a product of cellular metabolism, especially by the mitochondria. In addition to its roles as a dismutase, SOD1 is also known to regulate the expression of cellular stress response genes.

ALS/FTD patient alleles knocked into the endogenous *dSod1* locus share defects evident in AD suggesting related etiology A4V adults exhibit a shortened lifespan with males more strongly affected than females, with a median lifespan of 13 vs 35 days, respectively (Fig 5A). A4V adults (red) show a progressive decline in negative geotaxis/climbing when compared to wild type (WT) (light blue) (Fig 5B). The compromised neuronal function evident in G85R larvae results in reduced locomotor activity (Fig 5C) and a failure of adults to eclose (Fig 5D)²⁴. Live imaging of GFP tagged mitochondria (mitoGFP) in larval filets revealed a reduction in mitochondrial movement in both sensory (Fig 5E) and motor axons in G85R mutants, with significant reduction in total mitochondria²⁶. Defects in A4V climbing, and locomotion, eclosion and mitochondrial transport along axons in G85R are fully or partially suppressed by the genetic variant *tkt*^{d84}, an insertion in the *transketolase* (*tkt*) gene encoding the key enzyme in the non-oxidative PPP that coordinates flux through oxidative PPP, coupled with glycolysis, and nucleotide biosynthesis. In essence, Tkt acts as a rheostat controlling metabolic flux through these pathways, by catalyzing reversible reactions that provide the building blocks for sugars, nucleotides, lipids and amino acids. Given the high metabolic demands of neurons, our finding that *tkt* acts as a genetic suppressor across multiple models of ALS/FTD, including C9orf72-G4C2, TDP43 and FUS, suggested that increased flux through the PPP may restore neuron function through glucose metabolism and nucleotide biosynthesis. As such, as described below we intend to investigate how additional regulators of glycolysis, nucleotide/NAD metabolism and OXPHOS influence mitonuclear interactions.

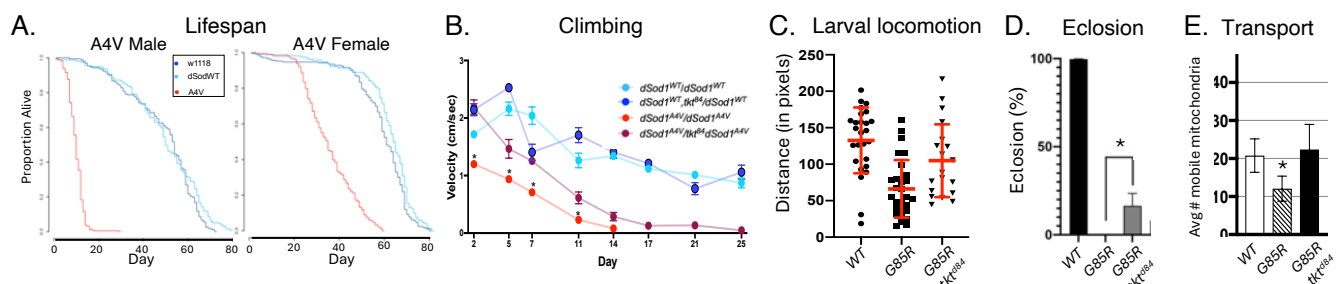


Fig 5. Neurodegeneration phenotypes of *dSod1* knock-in models. A. A4V adult lifespan, number dead counted daily, n=100/genotype/cage, 3 replicates. Survival curves by Kaplan-Meier method, Stats: Chi-square log rank test. B. Climbing velocity of adults of indicated genotypes measured over 17 days (n=60, p<0.01, ANOVA with Hochberg correction for multiple comparisons). C. Plot of distance traveled over 90s. D. Adult eclosion frequency (n>85, p<0.0001, Fisher's exact test). E. Quantification of mitochondria in MD-Gal4 UAS mitoGFP G85R, live imaging 400frames, 0.84 s/frame at A3/4, n=4. One-way ANOVA, Tukey's multiple comparison.

Neuronal compartment-specific reduction in mitochondrial content and network Both SOD1 models exhibit a progressive decline in mitochondria with a severe reduction in mitochondrial content in axons of adult A4V (Fig 6A). In G85R, the number of mitochondria at axon terminals are lower than in controls with no change in number in the cell body on MD (multidendritic) neurons, a population of cholinergic neurons that integrate position and other sensory cues (Fig 6B). The selective reduction of mitochondria at the axon terminal (synapse) is progressive with no difference in mid-3rd instar larvae but significant loss 12 hrs. later at a time when only the beginning of degeneration of neurons is

apparent^{24,26}. We determined the loss is not due to a general axonal transport defect, as the transport of other cargoes are unaffected in these neurons²⁶. Iijima-Ando (2009) observed the same preferential loss of mitochondria from different neuronal compartments in mushroom bodies of an A β 42 model with pan-neuronal (*elav-Gal4>UAS-A β 42*) or cholinergic (*Cha-Gal4>UAS-A β 42*) expression of mito-GFP^{27,28}. They also concluded that the reduction in mitochondria from axons and then dendrites was not due to a general disruption of microtubule-based transport. Instead, the defect in movement of mitochondria in these neurodegenerative models more likely reflects a dysfunctional organelle, whose role in OXPHOS and as the main source for ATP production is disrupted, failing to maintain energy homeostasis. Indeed, we found that mitochondria isolated from G85R larvae have lower levels of NADH, and both G85R and A4V show reduced levels of ATP. Furthermore, using an *in vivo* reporter for mitolysosomes (mitoQC)^{29,30} we measured higher levels of mitophagy at the axon termini of G85R consistent with a reduced number of mitochondria in this cellular compartment (Fig 6C).

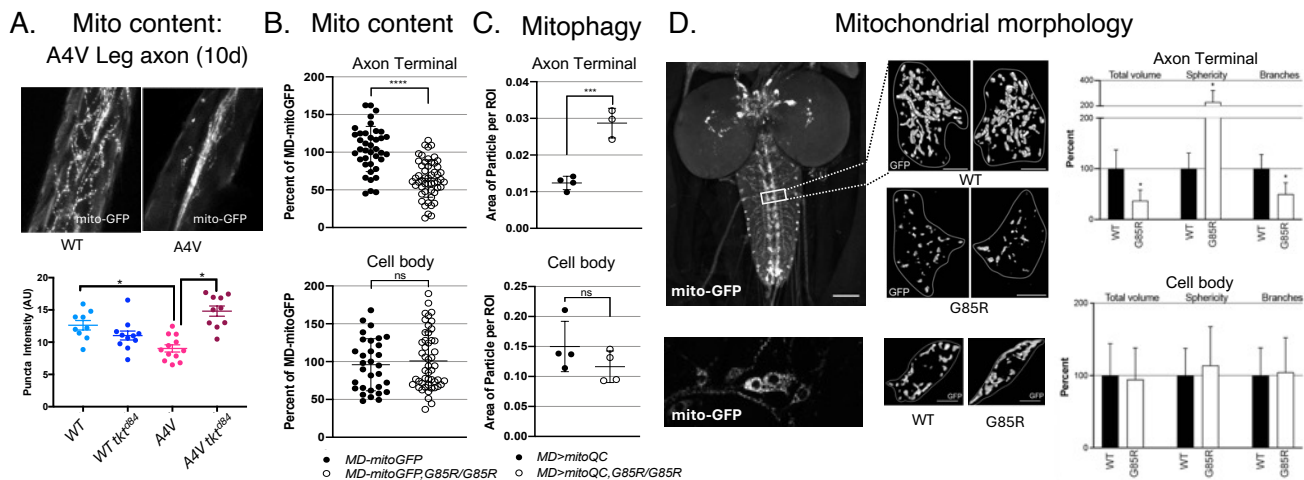


Fig 6 Mitochondrial defects associated with *dSod1* knock-in models. A. Top: mitoGFP in WT, WT tkt⁸⁵⁴, A4V and A4V tkt⁸⁵⁴ adult legs at 10days, OK371>mitoGFP. Bottom: Quantification of mitochondria using Fiji. B. Quantification of mito-GFP in G85R (n=52 larvae) as percentage of WT (n=39). C. Quantification of MD>mitoQC, mitolysosome particles normalized to synaptic (top) and cell body (bottom) areas. Student's t-test. D. MD-Gal4>mito-GFP Top: Ventral nerve cord, axon terminal (boxed). Bottom: MD cell bodies. 3D rendering of confocal Z stacks. Scale bar=50μm. Subset of quantified morphological parameters, Mito-Analyzer (Fiji plug-in Chaundry 2020). n= 10-18 larvae.

More detailed morphological studies revealed highly fragmented mitochondria at the axon terminal, with higher measures of sphericity and fewer branches, indicative of less networked mitochondria (Fig 6D)²⁶. Wang and Davis (2021) also found expressing A β 42 in the axons and dendrites of the mushroom body mitochondria became fragmented at an early age followed by an increase in autophagy and memory impairment at later ages²⁸. Our data coupled with that of Wang and Davis is consistent with emerging evidence that mitochondrial dysfunction occurs early evidenced by organelle fragmentation, leading to further decline as proposed in the mitochondrial cascade hypothesis³¹⁻³³. A disruption in mitochondrial morphology has also been documented in animal models of tauopathy, specifically in the *Drosophila* model *elav-Gal4>UAS-tau^{R406W}* that replicates many features of human AD and related tauopathies (see refs^{22,34-37}). Similar to our finding that genetic manipulation of the mitochondrial fission factor Drp1 can restore mitochondria networks at the synapses of G85R MD neurons^{26,38} showed that *tau* expression altered actin-dependent localization of Drp1 resulting in morphological change to mitochondria^{22,36}.

As an unbiased means to identify modifiers of neurodegeneration, the Wharton lab has conducted several different genetic screens with G85R and C9orf72-G4C2, and tested each suppressor against the other ALS/FTD models, A4V, TDP43, and FUS, identifying a number of genetic variants that suppress models of all four disease-associated genes. A group of these suppressor genes encode enzymes linked to metabolic pathways linked to PPP. As noted above Tkt regulates flux through the PPP and demonstrates an ability to suppress multiple ALS/FTD model phenotypes. The expression of *Gapdh1*, the gene encoding glyceraldehyde-3-phosphate dehydrogenase (GAPDH), a key enzyme in the first payoff step of glycolysis, was found to be elevated in G85R and when knocked down a significant increase in G85R survival (76%) was observed with a restoration of mitochondrial transport and mitochondrial morphology (data not shown). Other suppressor genes correlated with the pathways most disrupted in our metabolomic analysis of G85R, namely nicotinate/nicotinamide and nucleotide

biosynthesis (Fig 7). Decreases in metabolites in the nicotinamide pathway, such as NR, NMN and NAD⁺ are evident as are shifts in purine metabolites (Fig 7).

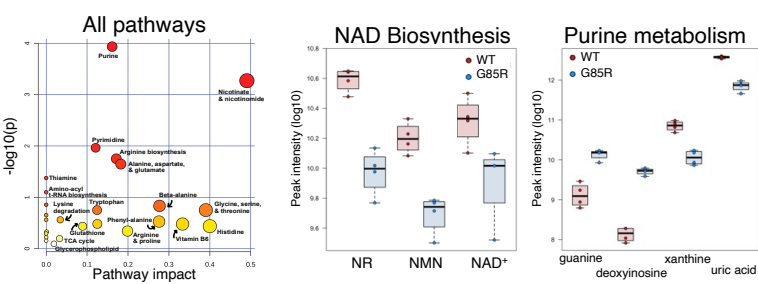


Fig 7. Metabolites altered in G85R compared to WT. Abundance of specific metabolites in NAD biosynthesis and purine metabolism.

We expanded our functional analysis to examine other genes that encode enzymes in PPP, as well as nucleotide/NAD biosynthesis (Fig 8) to test for their ability to influence neurodegeneration in all four models of ALS/FTD. In addition to *tkt*, we found *Taldo*, *Rpe*, and *Rpi* but not *Zw* (G6PD) or *Pgd* (6PGD) in PPP could suppress. *Prps*, *Dhod*, *e(r)*, *Paics*, *Nadk* and *Nmnat* in nucleotide/ NAD biosynthesis alleviated multiple neurodegeneration phenotypes associated with SOD1, TDP43, FUS, and C9orf72-G4C2 models (Zhou et al, manuscript in prep; Fig 8). Interestingly, disruptions in purine metabolism have been attributed to AD with a similar increase in guanine as we see, but a decrease in other metabolites such as xanthine³⁹ (Fig. 8). A number of reports have highlighted the role for NAD⁺ and related metabolites in AD and aging in general, with more studies investigating the potential benefits of NAD⁺ precursors as effective interventions for AD (reviewed in⁴⁰⁻⁴². As a representative of each major pathway, in Aim 2B we will test the effect of the different mitonuclear genomes on the ability of *Gapdh1*, *tkt*, *Paics* and *Nmnat* to suppress G85R, A4V, as well as Ab42 and tau^{R406W} associated phenotypes.

In addition to the defects in mitochondrial transport, morphology, and function we observed in our G85R and A4V models, our RNA-seq dataset for G85R revealed increased expression of a subset of genes that encode components of complex I, II, and IV, as well as Coenzyme Q, in the electron transport chain. We tested if the fragmented mitochondrial network at the G85R synapse could be ameliorated by a knock down of each of these genes, *NADH dehydrogenase 51-like1* (*ND51L1*), *succinate dehydrogenase subunit B-like* (*SdhBL*), *cytochrome c oxidase subunit 6A-like2* (*COX6A1*), and *coenzyme Q8* (*Coq8*). Indeed, we found significant rescue with a restoration of networked mitochondria at the axon terminals in G85R (Fig 9A,B). Furthermore, knock down of *SdhBL* increased the number of mobile mitochondria in G85R MD neurons²⁶ and in keeping with the observation that ETC complexes exhibit compensatory actions to maintain ETC-homoestasis⁴³, the downregulation of *SdhBL* (Complex II) led to upregulation of *ND51L1* (Complex I). Disruptions in OXPHOS will impact the production of reactive oxygen species (ROS). Oxidative stress has been implicated in many neurodegenerative diseases like ADRD, but little is known about quantitative changes *in vivo*, at the cellular level which is tightly linked to the redox state of the cell. We optimized the *in vivo*

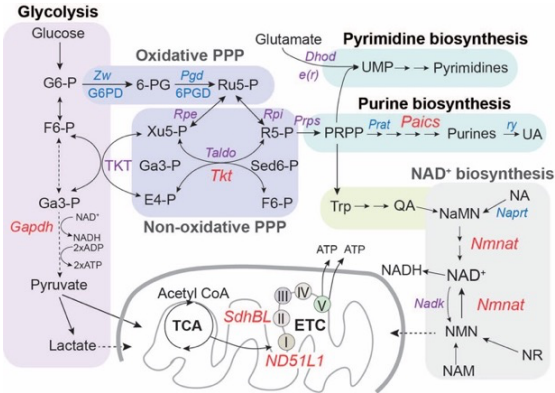


Fig 8. Suppressor genes (red,purple) encode enzymes in glycolysis, PPP, nucleotide, and NAD biosynthesis as well as subunits of ETC complexes. Gene tested that did not suppress ALS/FTD models.

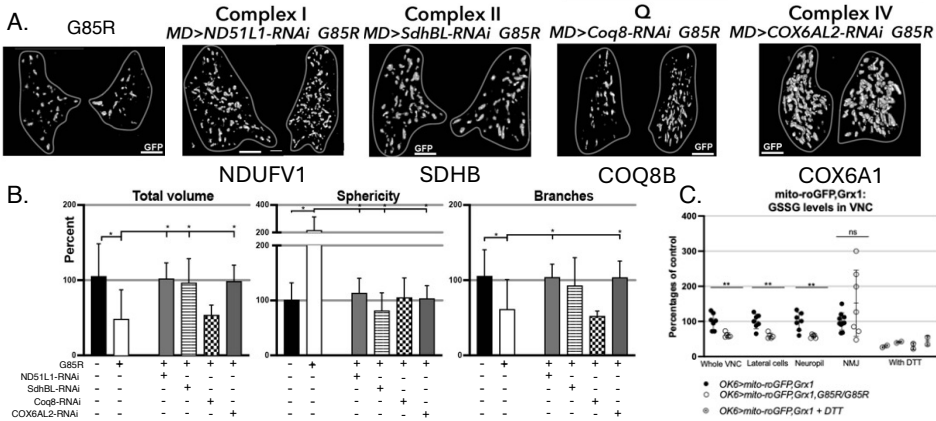


Fig 9 Knock-down of ETC components alleviates mitochondrial phenotypes of *dSod1* G85R. A 3D reconstructions of synaptic mitochondria at A2 of VNC – left and right side – for MD>mitoGFP G85R and genotypes listed for components of ETC complexes. B. Quantification of morphological parameters MitoAnalyzer (Fiji). One-way ANOVA with Tukey’s multiple comparison on normally distributed data. Scale bar 10um. C. Ratio of 405nm to 488nm fluorescence normalized to ROI and plotted as percentage of WT ratio. VNCs treated with DTT reductant to test specificity of signal. Student’s t-test.

mito-redox-GFP (mito-ro-GFP) biosensors for glutathione oxidation (UAS-mito-roGFP2-Grx1) and for H₂O₂ oxidation (UAS-mito-roGFP2-Orp1)⁴⁴⁻⁴⁶ and found a significant disruption in the ventral nerve cord (VNC) and brain of G85R but no change at the NMJ. These results indicate that the mitochondria cell bodies and dendrites of mutant neurons are unable to maintain the proper GSH/GSSG ratio, another measure of mitochondrial dysfunction.

2. Innovation

The majority of studies investigating causes of ADRD have focused on A β and Tau given the strong clinical evidence for amyloid plaques and neurofibrillary tangles in AD brains. The growing evidence that mitochondrial phenotypes are causes or consequences of these associations has refocused attention on mitochondrial genes. Mitochondria are by no means limited to ATP production through OXPHOS⁴⁷ as their role as a hub regulating redox state, balanced calcium signaling, trafficking and axonal transport, fission-fusion dynamics, and mitophagy are well established⁴⁸. This mitochondrial-nexus view has motivated genomic and proteomic screens for nuclear genes that regulate mitochondrial function⁴⁹⁻⁵². While there is a rich literature on seeking mtDNA associations with ADRD using case-control statistical analyses, the direct manipulation of mtDNA encoded genes in the interrogation of ADRD etiology is extremely rare. *A key innovation of the proposed research program is to use mtDNA genotypes as modifiers of ADRD gene effects. This provides a focused manipulation of the mitochondrial-nuclear interaction problem now believed to be a central factor in ADRD.*

A second major innovation is to leverage the power of the *Drosophila* genetic model of tissue specific genetic manipulations to provide precise control of the major candidate genes underlying ADRD in dissecting mitonuclear interactions. *Drosophila* studies have played important roles in validating and identifying ADRD genes in altered mitochondrial function. The extent of tissue-specific mtDNA effects is poorly understood but is known to be significant. *The ability to identify how distinct mtDNA backgrounds alter tissue specific transcriptional, metabolic and overall phenotypic effects of ADRD genes can discover new roles for genes, metabolites and organelle dynamics underlying disease states.*

A third major innovation of this work is our ability to probe the mitochondrial basis of genetic rescues of known ADRD genes. As presented above, genes that rescue the SOD models fall in several different metabolic pathways (carbohydrate, purine, OXPHOS) that intersect with mitochondrial function in different ways. The combined use of mtDNA backgrounds to alter these rescue effects can identify changes in metabolite levels that are known to be signaling molecules in mitochondrial-nuclear communication. *Thus, this proposal is innovative because it employs novel resources and analyses to connect nuclear and mitochondrial genotypes to pathways influencing ADRD.*

These studies will have several positive impacts on the field.

- 1) **We will identify genes and metabolites involved in mitonuclear communication in ADRD.**
- 2) **We will identify genes and metabolites that mediate genetic rescue of ADRD phenotypes.**
- 3) **We will identify targets for future analyses in vertebrate models and human brain tissue.**

The breadth of analyses in our *Drosophila* model will accelerate basic and translational research in ways that are prohibitive in vertebrate and clinical studies.

3. Approach

Drosophila is an incomparable system for elucidating the function of individual genes *in vivo*, defining the pathways in which they act, and revealing if and how they intersect. More than 60% of human disease genes are highly conserved in *Drosophila*, making *Drosophila* models of human disease particularly powerful for the elucidation of molecular and cellular dysfunctions⁵³⁻⁶⁰. The functional organization of the nervous system in *Drosophila* and mammals is remarkably similar enabling impactful studies of neurological disease^{54,61}. Coupled with its utility for pathway analysis and the near complete conservation of metabolic processes and organelle biology, *Drosophila* has recently proven to be especially powerful for addressing questions centered in cellular metabolism^{41,62-64}. The relative abundance of different metabolites is an indicator of the physiological status of a cell. Metabolic enzymes are the work horses driving biochemical reactions, yet precisely how their regulation impacts

metabolic pathways is still poorly understood⁶⁵. Mitochondria are now recognized as much more than ATP factories, as many metabolic pathways pass through mitochondria⁴⁷. The overall state of the organelle can thus influence broad aspects of cellular health. Manipulating the joint mitonuclear genetic influence on this metabolic flux can identify novel links between traditional ATP production and broader metabolic health. We use genetic manipulations in *Drosophila* to test hypotheses based on observations made from patients with ADRD, their cells, or mammalian models to provide a mechanistic understanding. We couple subcellular to behavioral phenotypic analyses, using *in vivo* reporters of cellular physiology, profiling of changes in metabolites and gene expression as a means to measure their response to specific genetic alterations. Such profiling will reveal the molecular underpinnings of the neuroprotective versus neurodegenerative state, providing a set of biomarkers that will be indicative of restored neural function.

Aim 1. Identify factors underlying ADRD neurodegeneration in disrupted mitonuclear genome pairs. We will identify (**Aim 1A**) and validate (**Aim 1B**) genes and metabolites critical for mitonuclear communication that underlie the defects associated with ADRD by quantifying altered neurodegenerative phenotypes, mitochondrial bioenergetics and gene expression in disrupted and intact mtDNA-nuclear gene pairs. Validation in Aim 1B will be accomplished by gene and tissue-specific manipulation in disrupted and intact mitonuclear genetic combinations.

Aim 1A1. Construct mitonuclear genotypes pairing mtDNAs with nuclear constructs expressing ADRD models. The first step in pursuing the goals of Aim 1 is to build the genetic stocks necessary to manipulate joint mitochondrial and nuclear expression of the ADRD models. This involves the use of the bipartite Gal4–UAS system in which the different mitochondrial DNAs will be placed onto four different tissue-specific Gal4 drivers which will be crossed with UAS stocks to express the ADRD models, Ab42 and tauR406W^{21,22}. The mitochondrial Gal4 stocks are shown in the top half of Table 1. The UAS-ADRD models, shown in Table 2, will be compared to their controls, i.e., UAS-A β 40 and UAS-tau^{WT}. Two mtDNAs are from *D. melanogaster* (*Dm-OR*, *Dm-Zim*), which provide the ‘intact’ mitonuclear combination, and two are from *D. simulans* (*Ds-sm21*, *Ds-sil*) providing the ‘disrupted’ mitonuclear combination (see Figure 1 above). All lines are on a *w*¹¹¹⁸ background and each Gal4 transgene is marked with a mini-*w*⁺ construct allowing for recovery of the Gal4 based on a pigmented eye. To facilitate maintaining the nuclear background originating in the current mitonuclear combinations, we will make use of T2:3 balancer chromosome in the first cross such that we will recover the 2nd and 3rd chromosomes from the mitonuclear line in the first progeny. Subsequent crosses using males that do not undergo recombination will allow us to minimize heterozygosity in the final mito-Gal4 lines generated.

In addition to the A β 42 and tau^{R406W} models that involve overexpression of human disease genes via the Gal4-UAS system, we will introduce three alleles of *dSod1* onto the same four mtDNA backgrounds. The two knock-in patient alleles (G85R and A4V) are germline mutations generated using CRISPR-Cas9 editing and therefore, do not require a Gal4 driver to be expressed. The *dSod1*^{WT} allele is the control of the introduction of silent mutations to destroy PAM sites necessary for CRISPR-Cas9 editing. All alleles were generated on the same *w*¹¹¹⁸ background. One advantage of these ADRD models is that whole animal phenotypes can be quantified. Gal4 drivers will be used to express reporter genes such as UAS-mitoGFP and UAS-mitoQC, for the *in vivo* visualization of mitochondria and mitophagy, respectively. As a result, the *dSod1* stocks require a different set of crosses, described in Tables 3 and 4. When generating each *dSod1* allele a P3-dsRed cassette was introduced in an intergenic region adjacent to *dSod1* that expresses dsRed in both larval, pupal and adult tissues allowing for identification of the *dSod1* allele in progeny at multiple stages. The *dSod1* alleles are not marked with mini-*w*⁺ allowing us to follow Gal4 transgenes in addition to the *dSod1* alleles. The genotype notations for stocks listed in the tables are: *mtDNA* ; *Xchr* ; *2ndchr* ; *3rdchr*.

Aim 1A2. To quantify phenotypes generated by the disrupted mitonuclear combinations in an ADRD context, we will cross males from the *UAS-A β* and *tau* lines on the left margin of **Table 2** to the mtDNA-Gal4 stocks generated and listed in **Table 1**. These F1 genotypes shown in **Table 2** will provide the animals to measure the suite of phenotypes that will provide a robust assessment of conditions related

to ADRD. Note that *dSod1* genotypes require different crosses, shown in Table 3 and 4 below. **Phenotypic assays.** We will quantify 1) whole animal phenotypes, 2) mitochondrial content and morphology and 3) transcriptomic and metabolomic profiles, for both females and males, in each mitonuclear genotype. The whole animal phenotypes include survival (eclosion), climbing, and lifespan which are well documented readouts of neurodegeneration. Mitochondrial content and morphology will be quantified by the presence of *UAS-mitoGFP*. The results from these assays will be used to prioritize specific subsets of the mitonuclear genotypes to be chosen for RNA-seq and metabolomics. It is prohibitively expensive to carry out these assays on all genotypes, and the 'omics data sets will be more informative when applied to mitonuclear genotypes with the suite of organismal and mitochondrial phenotypes most relevant to ADRD.

All such phenotypic assays have been performed previously using the same *UAS-Aβ42* and *UAS-*tau*^{R406W}* lines^{66,27,28,38,67,68}

driven by *elav-Gal4*⁶⁹ in all neurons. These assays can be done on all genotypes, and both the Rand and Wharton labs have extensive experience in their quantification^{13,24-26}. Visualization of mitochondria in the resulting progeny is possible in mushroom body cells as shown by^{28,38} for *tau*^{R406W} and Aβ42, respectively. Mitochondrial content and morphology will be assessed while other in vivo biosensors such as

UAS-mitoQC, UAS-mito-roGFP, UAS-SoNaR, and UAS-AT1.03NL will be used if warranted to assess mitophagy, redox state, NADH/NAD⁺ ratio, and ATP levels, respectively^{70,71}. The Wharton lab has used these sensors previously (see Fig 6&9 above) and has the expertise to perform the required quantitative imaging²⁶. Additional assays for general levels of oxidative stress can be determined by dihydroethidium (DHE) staining^{38,66} or H2DCFDA (Molecular Probes C6827) staining, fluorescent probes to measure ROS levels. In addition, the levels and aggregation of Aβ42 in different mitonuclear backgrounds will be determined using anti-Aβ42 antibody (Santa Cruz Biotechnology)⁶⁶. The Ab model is also amenable to tests of learning and memory²⁸. Dr. Karla Kaun, an expert in developing and measuring complex behaviors, such as remembering, and as our scientific next-door neighbor, we look forward to exploring behavioral assays of our altered mito-ADRD models.

The two 'omics analyses (RNA-seq and metabolomics) can be done using the same genotypes used for phenotyping the Gal4-UAS models, as the expression is in tissues that can be sampled in bulk. The Rand lab has considerable experience with RNAseq and metabolomics analyses using mitonuclear genotypes^{10,14,15,17}. These data will test our central hypothesis that distinct mitonuclear genotypes generate altered gene expression and metabolite profiles via the action of key signaling molecules that mediate proper mitonuclear communication. There is growing evidence for this causal, apparently 'epigenetic' relationship in ADRD models^{3,19}. Notably, no study has performed such analyses where mtDNA and nuclear genotypes are manipulated in factorial designs as a means to identify how altered communication alters the impact of these signaling molecules.

Table 1. Mitonuclear Gal4 Driver stocks and *dSod1* germline mutant stocks

Nuclear genome	w ¹¹¹⁸			
	Dm-OR	Dm-Zim	Ds-sm21	Ds-sil
	Intact		Disrupted	
<i>elav-Gal4</i>	OR; <i>elavG4</i> ;;	Zim; <i>elavG4</i> ;;	sm21; <i>elavG4</i> ;;	sil; <i>elavG4</i> ;;
MD-Gal4	OR;;MDG4;	Zim;;MDG4;	sm21;;MDG4;	sil;;MDG4;
OK371-Gal4	OR;;OK371G4;	Zim;;OK371G4;	sm21;;OK371G4;	sil;;OK371G4;
OK107-Gal4	OR;;OK107G4	Zim;;OK107G4	sm21;;OK107G4	sil;;OK107G4
;; <i>dSod1</i> ^{WT}	OR;;; <i>dSod1</i> ^{WT}	Zim;;; <i>dSod1</i> ^{WT}	sm21;;; <i>dSod1</i> ^{WT}	sil;;; <i>dSod1</i> ^{WT}
;; <i>dSod1</i> ^{G85R}	OR;;G85R	Zim;;G85R	sm21;;G85R	sil;;G85R
;; <i>dSod1</i> ^{A4V}	OR;;A4V	Zim;;A4V	sm21;;A4V	sil;;A4V

Table 2. Generation of experimental progeny to assess mitonuclear in Aβ and tau

Male parent	Female parent w/ different mt-DNA			
	OR; <i>elavG4</i> ;;	Zim; <i>elavG4</i> ;;	sm21; <i>elavG4</i> ;;	sil; <i>elavG4</i> ;;
<i>UAS-mitoGFP</i> <i>UAS-Aβ40</i>	OR; <i>elavG4</i> ;;UAS- <i>mitoGFP</i> UAS-Aβ40	Zim; <i>elavG4</i> ;;UAS- <i>mitoGFP</i> UAS-Aβ40	sm21; <i>elavG4</i> ;;UAS- <i>mitoGFP</i> UAS-Aβ40	sil; <i>elavG4</i> ;;UAS- <i>mitoGFP</i> UAS-Aβ40
<i>UAS-mitoGFP</i> <i>UAS-Aβ42</i>	OR; <i>elavG4</i> ;;UAS- <i>mitoGFP</i> UAS-Aβ42	Zim; <i>elavG4</i> ;;UAS- <i>mitoGFP</i> UAS-Aβ42	sm21; <i>elavG4</i> ;;UAS- <i>mitoGFP</i> UAS-Aβ42	sil; <i>elavG4</i> ;;UAS- <i>mitoGFP</i> UAS-Aβ42
<i>UAS-mitoGFP</i> <i>UAS-tau</i> ^{WT}	OR; <i>elavG4</i> ;;UAS- <i>mitoGFP</i> UAS-tau ^{WT}	Zim; <i>elavG4</i> ;;UAS- <i>mitoGFP</i> UAS-tau ^{WT}	sm21; <i>elavG4</i> ;;UAS- <i>mitoGFP</i> UAS-tau ^{WT}	sil; <i>elavG4</i> ;;UAS- <i>mitoGFP</i> UAS-tau ^{WT}
<i>UAS-mitoGFP</i> <i>UAS-tau</i> ^{R406W}	OR; <i>elavG4</i> ;;UAS- <i>mitoGFP</i> UAS-tau ^{R406W}	Zim; <i>elavG4</i> ;;UAS- <i>mitoGFP</i> UAS-tau ^{R406W}	sm21; <i>elavG4</i> ;;UAS- <i>mitoGFP</i> UAS-tau ^{R406W}	sil; <i>elavG4</i> ;;UAS- <i>mitoGFP</i> UAS-tau ^{R406W}

Statistical analyses: As each phenotype will be quantified in all genotypes (or a subset for ‘omics), a common statistical framework will be applied to establish the significance of mtDNA, Nuclear and Interaction genetic effects on phenotypes. To test sex-specific effects, which are important in ADRD, we can add a term for Sex and explore all pairs of interactions. With replicates of each treatment the following linear models will be applied:

For each phenotype (transcript, or metabolite after normalization and filtering), we fit the following 2-factor model: **Model 1: Phenotype = m + mtDNA + Nuclear + mtDNAXNuclear + e**

Phenotypes with significant interaction terms in this model have a ‘mitonuclear’ genetic basis. To assess the sex-specific effects we fit a single 3-factor model to the data set containing both sexes: **Model 2: Phenotype = m + mtDNA + Nuclear + Sex + mtDNAXNuclear + mtDNAXSex + NuclearxSex + mtDNAXNuclearxSex + e**

Phenotypes that are sex specific are captured in the 2-way interaction terms and sex-specific mitonuclear effect are quantified in the 3-way interaction term. AD is more common in women than men and this quantitative approach will allow us to identify sets of phenotypes that co-occur in the two sexes. Interestingly, we have observed significant differences between the sexes in the *dSod1* models and we will explore this possibility in the Aβ and tau models.

Experimental progeny of homozygous knock-in *dSod1* alleles with each mtDNA type will be generated as indicated in Table 3 (green shading). We will assess any impacts of different mitonuclear communication in the context of the *dSod1* ADRD alleles by measuring eclosion frequency in G85R and A4V compared to WT, as well as climbing and lifespan in the A4V background compared to the WT control line. The eclosion, climbing and lifespan assays have been extremely valuable in our own labs, as well as of other labs in the neurodegeneration and aging fields, as a sensitive measure of whole-body health and function.

Table 3. Crosses to general animals for eclosion, lifespan, climbing in *Sod1* models

Male parent	Female parent w/ different mt-DNA			
	OR::; <i>dSod1</i> ^{WT}	Zim::; <i>dSod1</i> ^{WT}	sm21::; <i>dSod1</i> ^{WT}	sil::; <i>dSod1</i> ^{WT}
;; <i>dSod1</i> ^{WT}	OR::; <i>dSod1</i> ^{WT} / <i>dSod1</i> ^{WT}	Zim::; <i>dSod1</i> ^{WT} / <i>dSod1</i> ^{WT}	sm21::; <i>dSod1</i> ^{WT} / <i>dSod1</i> ^{WT}	sil::; <i>dSod1</i> ^{WT} / <i>dSod1</i> ^{WT}
;; <i>dSod1</i> ^{G85R}	OR::; <i>dSod1</i> ^{G85R}	Zim::; <i>dSod1</i> ^{G85R}	sm21::; <i>dSod1</i> ^{G85R}	sil::; <i>dSod1</i> ^{G85R}
;; <i>dSod1</i> ^{G85R} /TM6	OR::; <i>dSod1</i> ^{G85R} / <i>dSod1</i> ^{G85R}	Zim::; <i>dSod1</i> ^{G85R} / <i>dSod1</i> ^{G85R}	sm21::; <i>dSod1</i> ^{G85R} / <i>dSod1</i> ^{G85R}	sil::; <i>dSod1</i> ^{G85R} / <i>dSod1</i> ^{G85R}
;; <i>dSod1</i> ^{A4V}	OR::; <i>dSod1</i> ^{A4V}	Zim::; <i>dSod1</i> ^{A4V}	sm21::; <i>dSod1</i> ^{A4V}	sil::; <i>dSod1</i> ^{A4V}
;; <i>dSod1</i> ^{A4V}	OR::; <i>dSod1</i> ^{A4V} / <i>dSod1</i> ^{A4V}	Zim::; <i>dSod1</i> ^{A4V} / <i>dSod1</i> ^{A4V}	sm21::; <i>dSod1</i> ^{A4V} / <i>dSod1</i> ^{A4V}	sil::; <i>dSod1</i> ^{A4V} / <i>dSod1</i> ^{A4V}

Table 4. Crosses to generate genotypes for visualizing mitochondria in *dSod1* models

Male parent	Female parent w/ different mt-DNA			
	OR::; <i>dSod1</i> ^{WT}	Zim::; <i>dSod1</i> ^{WT}	sm21::; <i>dSod1</i> ^{WT}	sil::; <i>dSod1</i> ^{WT}
;;MDG4;UAS-mitoGFP <i>dSod1</i> ^{WT}	OR::MDG4;UAS-mitoGFP <i>dSod1</i> ^{WT} / <i>dSod1</i> ^{WT}	Zim::MDG4;UAS-mitoGFP <i>dSod1</i> ^{WT} / <i>dSod1</i> ^{WT}	sm21::MDG4;UAS-mitoGFP <i>dSod1</i> ^{WT} / <i>dSod1</i> ^{WT}	sil::MDG4;UAS-mitoGFP <i>dSod1</i> ^{WT} / <i>dSod1</i> ^{WT}
;;MDG4;UAS-mitoGFP <i>dSod1</i> ^{G85R} /TM6	OR::MDG4;UAS-mitoGFP <i>dSod1</i> ^{G85R} / <i>dSod1</i> ^{G85R}	Zim::MDG4;UAS-mitoGFP <i>dSod1</i> ^{G85R} / <i>dSod1</i> ^{G85R}	sm21::MDG4;UAS-mitoGFP <i>dSod1</i> ^{G85R} / <i>dSod1</i> ^{G85R}	sil::MDG4;UAS-mitoGFP <i>dSod1</i> ^{G85R} / <i>dSod1</i> ^{G85R}
;;OK371G4;UAS-mitoGFP <i>dSod1</i> ^{WT}	OR::OK371G4;UAS-mitoGFP <i>dSod1</i> ^{WT} / <i>dSod1</i> ^{WT}	Zim::OK371G4;UAS-mitoGFP <i>dSod1</i> ^{WT} / <i>dSod1</i> ^{WT}	sm21::OK371G4;UAS-mitoGFP <i>dSod1</i> ^{WT} / <i>dSod1</i> ^{WT}	sil::OK371G4;UAS-mitoGFP <i>dSod1</i> ^{WT} / <i>dSod1</i> ^{WT}
;;OK371G4;UAS-mitoGFP <i>dSod1</i> ^{A4V}	OR::OK371G4;UAS-mitoGFP <i>dSod1</i> ^{A4V} / <i>dSod1</i> ^{A4V}	Zim::OK371G4;UAS-mitoGFP <i>dSod1</i> ^{A4V} / <i>dSod1</i> ^{A4V}	sm21::OK371G4;UAS-mitoGFP <i>dSod1</i> ^{A4V} / <i>dSod1</i> ^{A4V}	sil::OK371G4;UAS-mitoGFP <i>dSod1</i> ^{A4V} / <i>dSod1</i> ^{A4V}

To quantify mitochondrial transport, content, and morphology we will use the UAS-mitoGFP marker in the mito-*Sod1* mutant background. Table 4 provides an example of crosses that will be done between males in each row to mito-*dSod1* female genotypes in each column. The crosses delineated in the top half of Table 4 will generate progeny to measure transport, content and morphology in MD neurons of G85R larvae as we have done previously²⁶. These neurons are cholinergic, neurons that have been shown to be preferentially affected in AD⁷² and they allow for detailed analysis of mitochondria in different subcellular compartments²⁶. The experimental progeny generated in the bottom half will be used to visualize mitochondria in axons in the adult legs, thoracic ganglia and brain. The survival over time of sensory cells using this Gal4 driver has been informative as to the toxicity of Aβ⁴²⁶⁷. We will start with the crosses shown in Table 4 to generate experimental progeny but having built the suite of mito-Gal4 and mito-*dSod1* stocks as outlined in Table 1, we will have the ability to examine the effect of broad pan neuronal expression, whole body as well as more detailed assessments of the incompatible mitonuclear backgrounds in the context of ADRD.

Aim 1B. Identify genes and metabolites critical for mitonuclear communication that underlie the defects associated with ADRD. A multitude of transcripts and metabolites show altered abundance in

ADRD genetic models and in patients compared to matched controls^{3,19}. Identifying these factors and which are the cause or consequence of the disease remains elusive. Aim 1A will identify those factors that are unique to the altered mitonuclear context of each ADRD model. This sub Aim seeks to validate the role of such factors through targeted manipulation of their abundance. For altered transcripts, this will require adding an RNAi or overexpression construct to the mitonuclear Gal4-UAS combination that modified the level of that transcript in the original assay. We will test the hypothesis that altering transcripts that were differentially expressed between intact and disrupted mitonuclear genotype pairs modifies the phenotypes originally associated with that pair of genotypes. In short, this is a modifier ‘screen’ of a select set of genotypes using specific candidate genes identified in the initial screen. For metabolites, this validation would require a construct that alters an enzyme upstream of that metabolite to alter its abundance, and knock-down or overexpression of that enzyme could achieve this goal. The construction of such Gal4-UAS genotypes can be done as we describe in Aim 2, in which such modifier constructs have already been built based on the *dSod1* model (e.g., Table 5). The expectation of these experiments is that reversing the originally-altered expression level of the newly discovered transcript will reverse the phenotypic effect. The statistical models described above can test the significance of these effects, using the 3-way model with the modifier in place of the ‘Sex’ term.

Aim 2. Identify factors affecting suppression of ADRD neurodegeneration in disrupted mitonuclear genome pairs. Aim 2A. We will identify mitonuclear

communication factors that alter the progression of ADRD by comparing disrupted and intact mitonuclear genotypes in the context of suppressed degeneration. The Wharton lab has identified ADRD suppressor genes that fall in different, but connected, biochemical pathways: glycolysis, pentose phosphate pathway (PPP), purine metabolism, and NAD biosynthesis (Fig 8; Table 5). These suppressors rescue both organismal (climbing, survival) and mitochondrial phenotypes (content and morphology). As these pathways include metabolites that pass through mitochondria, we will test the hypothesis that the genetic suppression process is sensitive to the mtDNA background (intact vs. disrupted). This will be achieved in a manner similar to Aim 1, but using genetic manipulation of the suppressor genes in the context of the ADRD model paired with different mtDNAs. **Table 6** provides an example of the crosses to obtain the desired experimental genotypes whereby *Nmnat* will be overexpressed, a condition that results in a significant suppression of early death and neurodegeneration.

The male parents carrying different UAS constructs for suppressors, GFP reporter, and ADRD model or control are listed in each row on the left of the table. The female parents carrying the different mtDNAs paired with the pan neuronal driver *elavGal4* are listed in each column at the top. The cell in each row shows the genotypes of the F1 offspring from the male x female cross. The top-left cell has this genotype: OR mtDNA; the pan neuronal driver *elavGal4*; the UAS-*Nmnat* suppressor; the UAS-mitoGFP for visualizing mitochondria; and the ADRD model (or control Aβ40). The remaining rows show additional ADRD model x suppressor combinations. As in Aim 1, the *Sod1* germline models require different crosses, so tests of suppressor genes on G85R and A4V would be done as shown in Table 4 but with a UAS-

Table 5. Suppressor gene constructs/mutants
PPP:
UAS- <i>tkt</i> -OE
<i>tktd84</i>
Glycolysis:
Gapdh1-RNAi (KD)
UAS-Gapdh1-G2285 (OE)
Purine metabolism:
UAS <i>Paics</i> -RNAi (KD)
NAD+ biosynthesis:
UAS- <i>Nmnat</i> (OE)
Complex I:
UAS-ND51L1-RNAi (KD)
Complex II:
UAS- <i>SdhBL</i> -RNAi (KD)
Fission/fusion:
DrpKG03815 (LOF)
UAS-Drp1 (OE)

Table 6. Crosses to generate mitonuclear ADRD models paired with specific suppressors

Male parent	Female parent w/ different mt-DNA			
	<i>OR;elavG4;;</i>	<i>Zim;elavG4;;</i>	<i>sm21;elavG4;;</i>	<i>sil;elavG4;;</i>
<i>UAS-Nmnat</i> ; <i>UAS-mitoGFP</i> <i>UAS-Aβ40</i>	<i>OR;elavG4;UAS-Nmnat</i> ; <i>UAS-mitoGFP UAS-Aβ40</i>	<i>Zim;elavG4; UAS-Nmnat</i> ; <i>UAS-mitoGFP UAS-Aβ40</i>	<i>sm21;elavG4; UAS-</i> <i>Nmnat; UAS-mitoGFP</i> <i>UAS-Aβ40</i>	<i>sil;elavG4; UAS-Nmnat</i> ; <i>UAS-mitoGFP UAS-Aβ40</i>
<i>UAS-Nmnat</i> ; <i>UAS-mitoGFP</i> <i>UAS-Aβ42</i>	<i>OR;elavG4; UAS-Nmnat</i> ; <i>UAS-mitoGFP UAS-Aβ42</i>	<i>Zim;elavG4; UAS-Nmnat</i> ; <i>UAS-mitoGFP UAS-Aβ42</i>	<i>sm21;elavG4; UAS-</i> <i>Nmnat; UAS-mitoGFP</i> <i>UAS-Aβ42</i>	<i>sil;elavG4; UAS-Nmnat</i> ; <i>UAS-mitoGFP UAS-Aβ42</i>
<i>UAS-Nmnat</i> ; <i>UAS-mitoGFP</i> <i>UAS-tau^{WT}</i>	<i>OR;elavG4; UAS-Nmnat</i> ; <i>UAS-mitoGFP UAS-tau^{WT}</i>	<i>Zim;elavG4; UAS-Nmnat</i> ; <i>UAS-mitoGFP UAS-tau^{WT}</i>	<i>sm21;elavG4; UAS-</i> <i>Nmnat; UAS-mitoGFP</i> <i>UAS-tau^{WT}</i>	<i>sil;elavG4; UAS-Nmnat</i> ; <i>UAS-mitoGFP UAS-tau^{WT}</i>
<i>UAS-Nmnat</i> ; <i>UAS-mitoGFP</i> <i>UAS-tau^{R406W}</i>	<i>OR;elavG4; UAS-Nmnat</i> ; <i>UAS-mitoGFP UAS-</i> <i>tau^{R406W}</i>	<i>Zim;elavG4; UAS-Nmnat</i> ; <i>UAS-mitoGFP UAS-</i> <i>tau^{R406W}</i>	<i>sm21;elavG4; UAS-</i> <i>Nmnat; UAS-mitoGFP</i> <i>UAS-tau^{R406W}</i>	<i>sil;elavG4; UAS-Nmnat</i> ; <i>UAS-mitoGFP UAS-</i> <i>tau^{R406W}</i>

Suppressor like *UAS-Nmnat*.

Aim 2B. Define the mechanistic basis underlying the suppression of ADRD phenotypes through manipulation of transcript and metabolite profiles of mutant and genetically suppressed ADRD genotypes in disrupted and intact mitonuclear combinations. This sub Aim mirrors that for Aim 1B, and is important in validating the findings of the role of mitonuclear communication in suppression. Our central hypothesis is that metabolites acting as signaling molecules mediating mitonuclear communication play active roles in the mechanisms of ADRD suppression. Aim 2A will identify transcripts and metabolites that are altered in the suppressed context of the ADRD model. This sub Aim seeks to validate the role of these factors by altering their abundance in the suppressed ADRD mitonuclear genotypes. We will test two alternative hypotheses regarding the role of these factors in suppression: 1) that the factor is necessary for the mechanism of action of the suppressor gene, 2) that the factor is sufficient to act as a suppressor on its own. A test of hypothesis 1 will require adding a UAS construct that knocks down (RNAi) or overexpresses the novel gene in the mitonuclear Gal4-UAS combination showing suppression of the ADRD phenotypes (as defined in Table 6). A test of hypothesis 2 will require adding a UAS construct that knocks down (RNAi) or overexpresses the novel gene in the ADRD model without the suppressor. The outcome of these experiments will determine if the novel mitonuclear suppressor factor acts in a common, or distinct, pathway as the original suppressor. For metabolites, this validation would require a construct that alters an enzyme upstream of that metabolite to alter its abundance, and knock-down or overexpression of that enzyme could achieve this goal. The construction of such Gal4-UAS genotypes can be done as we describe in Aim 2A. The expectation of these experiments is that reversing the originally-altered expression level of the newly discovered transcript will reverse the phenotypic effect. The statistical models described above can test the significance of these effects, using the 3-way model with the modifier in place of the ‘Sex’ term.

Expected outcomes and alternative approaches. The expected outcomes of these Aims are the identification of the mitonuclear genetic basis underlying biochemical networks governing the degenerative nature of ADRD. Our findings will accelerate the development of mammalian models of mitonuclear communication in ADRD and can lead to more efficient analyses of precious patient samples in the search for effective therapies. If we run into a problem with viability or sterility when both Gal4 and UAS-suppressor are in the same animal then we would need to introgress a Gal4;G85R into the 4 mito backgrounds to produce stocks from which we will derive females for the crosses to generate an experimental animal that is: mt-DNA;; X-Gal4/UAS-Supp; G85R/G85R. Should elav-Gal4 result in lethality given its early expression in the embryo from the time of neuronal differentiation, we will use neuronal synaptobrevin-Gal4 (n-Syb-Gal4), a pan neuronal driver whose expression begins later during the larval period with higher levels of expression in the adult ⁷³.

Timeline. The Timeline table provides a general overview of our plans for this research. We anticipate that a few years will be needed to build the genotypes, with assays underway as they are constructed. Validation of findings in each Aim will require additional genotypes and phenotypes, but a smaller set.

Timeline of Projects	Year 1	Year 2	Year 3	Year 4	Year 5
Aim 1: Mitonuclear ADRD pnenotypes					
Aim 1A1: Genotype construction					
Aim 1A2: Phenotypes, 'omics					
Aim 1B: Validation genotypes & phenotypes					
Aim 2: Mitonuclear ADRD supression					
Aim 2A: Genotype construction					
Aim 2B: Phenotype analyses					
Publication					
Statistical analyses and writing					
Manuscript preparation					

Rigor and reproducibility. All of these experiments will be repeated in multiple blocks to confirm reproducibility before publishing. Several of these proposed experiments address reproducing published ideas with novel designs, which addresses reproducibility between laboratories.

Sex and a biological variable. All of the experiments in the proposed research addresses reproducibility of sex-effects in general, and statistical analyses are provided to quantify these effects.

BIBLIOGRAPHY & REFERENCES CITED

- 1 2024 Alzheimer's disease facts and figures. *Alzheimers Dement* **20**, 3708-3821 (2024).
<https://doi.org/10.1002/alz.13809>
- 2 Yin, K. F. *et al.* Identification of Potential Causal Genes for Neurodegenerative Diseases by Mitochondria-Related Genome-Wide Mendelian Randomization. *Mol Neurobiol* (2024).
<https://doi.org/10.1007/s12035-024-04528-3>
- 3 Marmolejo-Garza, A. *et al.* Transcriptomic and epigenomic landscapes of Alzheimer's disease evidence mitochondrial-related pathways. *Biochim Biophys Acta Mol Cell Res* **1869**, 119326 (2022). <https://doi.org/10.1016/j.bbamcr.2022.119326>
- 4 Norambuena, A. *et al.* A novel lysosome-to-mitochondria signaling pathway disrupted by amyloid-beta oligomers. *EMBO J* **37** (2018). <https://doi.org/10.15252/emboj.2018100241>
- 5 Norambuena, A. *et al.* SOD1 mediates lysosome-to-mitochondria communication and its dysregulation by amyloid-beta oligomers. *Neurobiol Dis* **169**, 105737 (2022).
<https://doi.org/10.1016/j.nbd.2022.105737>
- 6 Rand, D. M., Fry, A. & Sheldahl, L. Nuclear-mitochondrial epistasis and drosophila aging: introgression of *Drosophila simulans* mtDNA modifies longevity in *D. melanogaster* nuclear backgrounds. *Genetics* **172**, 329-341 (2006). <https://doi.org/10.1534/genetics.105.046698>
- 7 Montooth, K. L., Meiklejohn, C. D., Abt, D. N. & Rand, D. M. Mitochondrial-nuclear epistasis affects fitness within species but does not contribute to fixed incompatibilities between species of *Drosophila*. *Evolution* **64**, 3364-3379 (2010). <https://doi.org/10.1111/j.1558-5646.2010.01077.x>
- 8 Meiklejohn, C. D. *et al.* An Incompatibility between a mitochondrial tRNA and its nuclear-encoded tRNA synthetase compromises development and fitness in *Drosophila*. *PLoS Genet* **9**, e1003238 (2013). <https://doi.org/10.1371/journal.pgen.1003238>
- 9 Zhu, C. T., Ingelmo, P. & Rand, D. M. GxGxE for lifespan in *Drosophila*: mitochondrial, nuclear, and dietary interactions that modify longevity. *PLoS Genet* **10**, e1004354 (2014).
<https://doi.org/10.1371/journal.pgen.1004354>
- 10 Villa-Cuesta, E., Holmbeck, M. A. & Rand, D. M. Rapamycin increases mitochondrial efficiency by mtDNA-dependent reprogramming of mitochondrial metabolism in *Drosophila*. *J Cell Sci* **127**, 2282-2290 (2014). <https://doi.org/10.1242/jcs.142026>
- 11 Mossman, J. A., Biancani, L. M., Zhu, C. T. & Rand, D. M. Mitonuclear Epistasis for Development Time and Its Modification by Diet in *Drosophila*. *Genetics* **203**, 463-484 (2016).
<https://doi.org/10.1534/genetics.116.187286>
- 12 Sujkowski, A. *et al.* Mito-nuclear interactions modify *Drosophila* exercise performance. *Mitochondrion* **47**, 188-205 (2019). <https://doi.org/10.1016/j.mito.2018.11.005>
- 13 Spierer, A. N., Yoon, D., Zhu, C. T. & Rand, D. M. FreeClimber: automated quantification of climbing performance in *Drosophila*. *J Exp Biol* **224** (2021). <https://doi.org/10.1242/jeb.229377>
- 14 Mossman, J. A. *et al.* Mitonuclear Interactions Mediate Transcriptional Responses to Hypoxia in *Drosophila*. *Mol Biol Evol* **34**, 447-466 (2017). <https://doi.org/10.1093/molbev/msw246>
- 15 Santiago, J. C. *et al.* Mitochondrial genotype alters the impact of rapamycin on the transcriptional response to nutrients in *Drosophila*. *BMC Genomics* **22**, 213 (2021).
<https://doi.org/10.1186/s12864-021-07516-2>
- 16 Rand, D. M., Mossman, J. A., Spierer, A. N. & Santiago, J. A. Mitochondria as environments for the nuclear genome in *Drosophila*: mitonuclear GxGxE. *J Hered* **113**, 37-47 (2022).
<https://doi.org/10.1093/jhered/esab066>

- 17 Raynes, Y., Santiago, J. C., Lemieux, F. A., Darwin, L. & Rand, D. M. Sex, tissue, and mitochondrial interactions modify the transcriptional response to rapamycin in *Drosophila*. *BMC Genomics* **25**, 766 (2024). <https://doi.org/10.1186/s12864-024-10647-x>
- 18 Villa-Cuesta, E., Fan, F. & Rand, D. M. Rapamycin reduces *Drosophila* longevity under low nutrition. *IOSR J Pharm* **4**, 43-51 (2014). <https://doi.org/10.9790/3013-0408043051>
- 19 Nativio, R. *et al.* An integrated multi-omics approach identifies epigenetic alterations associated with Alzheimer's disease. *Nat Genet* **52**, 1024-1035 (2020). <https://doi.org/10.1038/s41588-020-0696-0>
- 20 Shen, K. *et al.* The germline coordinates mitokine signaling. *Cell* **187**, 4605-4620 e4617 (2024). <https://doi.org/10.1016/j.cell.2024.06.010>
- 21 Jonson, M., Pokrzywa, M., Starkenberg, A., Hammarstrom, P. & Thor, S. Systematic Aβ Analysis in *Drosophila* Reveals High Toxicity for the 1-42, 3-42 and 11-42 Peptides, and Emphasizes N- and C-Terminal Residues. *PLoS One* **10**, e0133272 (2015). <https://doi.org/10.1371/journal.pone.0133272>
- 22 Wittmann, C. W. *et al.* Tauopathy in *Drosophila*: neurodegeneration without neurofibrillary tangles. *Science* **293**, 711-714 (2001). <https://doi.org/10.1126/science.1062382>
- 23 Juneja, T., Pericak-Vance, M. A., Laing, N. G., Dave, S. & Siddique, T. Prognosis in familial amyotrophic lateral sclerosis: progression and survival in patients with glu100gly and ala4val mutations in Cu,Zn superoxide dismutase. *Neurology* **48**, 55-57 (1997). <https://doi.org/10.1212/wnl.48.1.55>
- 24 Held, A. *et al.* Circuit Dysfunction in *SOD1-ALS* Model First Detected in Sensory Feedback Prior to Motor Neuron Degeneration Is Alleviated by BMP Signaling. *The Journal of Neuroscience* **39**, 2347-2364 (2019). <https://doi.org/10.1523/JNEUROSCI.1771-18.2019>
- 25 Şahin, A. *et al.* Human *SOD1* ALS Mutations in a *Drosophila* Knock-In Model Cause Severe Phenotypes and Reveal Dosage-Sensitive Gain- and Loss-of-Function Components. *Genetics* **205**, 707-723 (2017). <https://doi.org/10.1534/genetics.116.190850>
- 26 Nemtsova, Y., Steinert, B. L. & Wharton, K. A. Compartment specific mitochondrial dysfunction in *Drosophila* knock-in model of ALS reversed by altered gene expression of OXPHOS subunits and pro-fission factor Drp1. *Mol Cell Neurosci* **125**, 103834 (2023). <https://doi.org/10.1016/j.mcn.2023.103834>
- 27 Iijima-Ando, K. *et al.* Mitochondrial mislocalization underlies Aβ42-induced neuronal dysfunction in a *Drosophila* model of Alzheimer's disease. *PLoS One* **4**, e8310 (2009). <https://doi.org/10.1371/journal.pone.0008310>
- 28 Wang, X. & Davis, R. L. Early Mitochondrial Fragmentation and Dysfunction in a *Drosophila* Model for Alzheimer's Disease. *Mol Neurobiol* **58**, 143-155 (2021). <https://doi.org/10.1007/s12035-020-02107-w>
- 29 Lee, J. J. *et al.* Basal mitophagy is widespread in *Drosophila* but minimally affected by loss of Pink1 or parkin. *Journal of Cell Biology* **217**, 1613-1622 (2018). <https://doi.org/10.1083/jcb.201801044>
- 30 Montava-Garriga, L., Singh, F., Ball, G. & Ganley, I. G. Semi-automated quantitation of mitophagy in cells and tissues. *Mechanisms of Ageing and Development* **185**, 111196 (2020). <https://doi.org/10.1016/j.mad.2019.111196>
- 31 Swerdlow, R. H. & Khan, S. M. A "mitochondrial cascade hypothesis" for sporadic Alzheimer's disease. *Med Hypotheses* **63**, 8-20 (2004). <https://doi.org/10.1016/j.mehy.2003.12.045>

- 32 Perez Ortiz, J. M. & Swerdlow, R. H. Mitochondrial dysfunction in Alzheimer's disease: Role in pathogenesis and novel therapeutic opportunities. *Br J Pharmacol* **176**, 3489-3507 (2019). <https://doi.org/10.1111/bph.14585>
- 33 Cenini, G. & Voos, W. Mitochondria as Potential Targets in Alzheimer Disease Therapy: An Update. *Front Pharmacol* **10**, 902 (2019). <https://doi.org/10.3389/fphar.2019.00902>
- 34 Jackson, G. R. *et al.* Human wild-type tau interacts with wingless pathway components and produces neurofibrillary pathology in *Drosophila*. *Neuron* **34**, 509-519 (2002). [https://doi.org/10.1016/s0896-6273\(02\)00706-7](https://doi.org/10.1016/s0896-6273(02)00706-7)
- 35 Nishimura, I., Yang, Y. & Lu, B. PAR-1 kinase plays an initiator role in a temporally ordered phosphorylation process that confers tau toxicity in *Drosophila*. *Cell* **116**, 671-682 (2004). [https://doi.org/10.1016/s0092-8674\(04\)00170-9](https://doi.org/10.1016/s0092-8674(04)00170-9)
- 36 Khurana, V. *et al.* TOR-mediated cell-cycle activation causes neurodegeneration in a *Drosophila* tauopathy model. *Curr Biol* **16**, 230-241 (2006). <https://doi.org/10.1016/j.cub.2005.12.042>
- 37 Iijima, K., Gatt, A. & Iijima-Ando, K. Tau Ser262 phosphorylation is critical for Abeta42-induced tau toxicity in a transgenic *Drosophila* model of Alzheimer's disease. *Hum Mol Genet* **19**, 2947-2957 (2010). <https://doi.org/10.1093/hmg/ddq200>
- 38 DuBoff, B., Gotz, J. & Feany, M. B. Tau promotes neurodegeneration via DRP1 mislocalization in vivo. *Neuron* **75**, 618-632 (2012). <https://doi.org/10.1016/j.neuron.2012.06.026>
- 39 Ansoleaga, B. *et al.* Deregulation of purine metabolism in Alzheimer's disease. *Neurobiol Aging* **36**, 68-80 (2015). <https://doi.org/10.1016/j.neurobiolaging.2014.08.004>
- 40 Wang, M. *et al.* Transformative Network Modeling of Multi-omics Data Reveals Detailed Circuits, Key Regulators, and Potential Therapeutics for Alzheimer's Disease. *Neuron* **109**, 257-272 e214 (2021). <https://doi.org/10.1016/j.neuron.2020.11.002>
- 41 Li, F., Wu, C. & Wang, G. Targeting NAD Metabolism for the Therapy of Age-Related Neurodegenerative Diseases. *Neurosci Bull* **40**, 218-240 (2024). <https://doi.org/10.1007/s12264-023-01072-3>
- 42 Alghamdi, M. & Braidy, N. Supplementation with NAD⁺ Precursors for Treating Alzheimer's Disease: A Metabolic Approach. *J Alzheimers Dis* **101**, S467-S477 (2024). <https://doi.org/10.3233/JAD-231277>
- 43 Weinrich, T. W. *et al.* A day in the life of mitochondria reveals shifting workloads. *Scientific Reports* **9**, 13898 (2019). <https://doi.org/10.1038/s41598-019-48383-y>
- 44 Houlihan, K. L. *et al.* Folic Acid Improves Parkin-Null *Drosophila* Phenotypes and Transiently Reduces Vulnerable Dopaminergic Neuron Mitochondrial Hydrogen Peroxide Levels and Glutathione Redox Equilibrium. *Antioxidants (Basel)* **11** (2022). <https://doi.org/10.3390/antiox11102068>
- 45 Krzystek, T. J. *et al.* Differential mitochondrial roles for alpha-synuclein in DRP1-dependent fission and PINK1/Parkin-mediated oxidation. *Cell Death Dis* **12**, 796 (2021). <https://doi.org/10.1038/s41419-021-04046-3>
- 46 Albrecht, Simone C., Barata, Ana G., Großhans, J., Teleman, Aurelio A. & Dick, Tobias P. In Vivo Mapping of Hydrogen Peroxide and Oxidized Glutathione Reveals Chemical and Regional Specificity of Redox Homeostasis. *Cell Metabolism* **14**, 819-829 (2011). <https://doi.org/10.1016/j.cmet.2011.10.010>
- 47 Raimundo, N. Mitochondrial pathology: stress signals from the energy factory. *Trends Mol Med* **20**, 282-292 (2014). <https://doi.org/10.1016/j.molmed.2014.01.005>

- 48 Nixon, R. A. & Yang, D. S. Autophagy failure in Alzheimer's disease--locating the primary defect. *Neurobiol Dis* **43**, 38-45 (2011). <https://doi.org/10.1016/j.nbd.2011.01.021>
- 49 Dillin, A. *et al.* Rates of behavior and aging specified by mitochondrial function during development. *Science* **298**, 2398-2401 (2002). <https://doi.org/10.1126/science.1077780>
- 50 Lee, S. S. *et al.* A systematic RNAi screen identifies a critical role for mitochondria in *C. elegans* longevity. *Nat Genet* **33**, 40-48 (2003). <https://doi.org/10.1038/ng1056>
- 51 Pagliarini, D. J. *et al.* A mitochondrial protein compendium elucidates complex I disease biology. *Cell* **134**, 112-123 (2008). <https://doi.org/10.1016/j.cell.2008.06.016>
- 52 Kohda, M. *et al.* A Comprehensive Genomic Analysis Reveals the Genetic Landscape of Mitochondrial Respiratory Chain Complex Deficiencies. *PLoS Genet* **12**, e1005679 (2016). <https://doi.org/10.1371/journal.pgen.1005679>
- 53 Jeon, Y., Lee, J. H., Choi, B., Won, S. Y. & Cho, K. S. Genetic Dissection of Alzheimer's Disease Using *Drosophila* Models. *Int J Mol Sci* **21** (2020). <https://doi.org/10.3390/ijms21030884>
- 54 Varte, V., Munkelwitz, J. W. & Rincon-Limas, D. E. Insights from *Drosophila* on Abeta- and tau-induced mitochondrial dysfunction: mechanisms and tools. *Front Neurosci* **17**, 1184080 (2023). <https://doi.org/10.3389/fnins.2023.1184080>
- 55 Reiter, L. T., Potocki, L., Chien, S., Gribskov, M. & Bier, E. A systematic analysis of human disease-associated gene sequences in *Drosophila melanogaster*. *Genome Res* **11**, 1114-1125 (2001). <https://doi.org/10.1101/gr.169101>
- 56 Lloyd, T. E. & Taylor, J. P. Flightless flies: *Drosophila* models of neuromuscular disease. *Ann N Y Acad Sci* **1184**, e1-20 (2010). <https://doi.org/10.1111/j.1749-6632.2010.05432.x>
- 57 Vidal, M. & Cagan, R. L. *Drosophila* models for cancer research. *Curr Opin Genet Dev* **16**, 10-16 (2006). <https://doi.org/10.1016/j.gde.2005.12.004>
- 58 McGurk, L., Berson, A. & Bonini, N. M. *Drosophila* as an In Vivo Model for Human Neurodegenerative Disease. *Genetics* **201**, 377-402 (2015). <https://doi.org/10.1534/genetics.115.179457>
- 59 Ugur, B., Chen, K. & Bellen, H. J. *Drosophila* tools and assays for the study of human diseases. *Dis Model Mech* **9**, 235-244 (2016). <https://doi.org/10.1242/dmm.023762>
- 60 Sonoshita, M. & Cagan, R. L. Modeling Human Cancers in *Drosophila*. *Curr Top Dev Biol* **121**, 287-309 (2017). <https://doi.org/10.1016/bs.ctdb.2016.07.008>
- 61 Okay, Z. & Hassan, B. A. Genetic approaches in *Drosophila* for the study neurodevelopmental disorders. *Neuropharmacology* **68**, 150-156 (2013). <https://doi.org/10.1016/j.neuropharm.2012.09.007>
- 62 Verstreken, P. *et al.* Synaptic mitochondria are critical for mobilization of reserve pool vesicles at *Drosophila* neuromuscular junctions. *Neuron* **47**, 365-378 (2005). <https://doi.org/10.1016/j.neuron.2005.06.018>
- 63 Hwa, J. J., Hiller, M. A., Fuller, M. T. & Santel, A. Differential expression of the *Drosophila* mitofusin genes fuzzy onions (*fzo*) and *dmfn*. *Mech Dev* **116**, 213-216 (2002). [https://doi.org/10.1016/s0925-4773\(02\)00141-7](https://doi.org/10.1016/s0925-4773(02)00141-7)
- 64 Cox, J. E., Thummel, C. S. & Tennessen, J. M. Metabolomic Studies in *Drosophila*. *Genetics* **206**, 1169-1185 (2017). <https://doi.org/10.1534/genetics.117.200014>
- 65 Yellen, G. Fueling thought: Management of glycolysis and oxidative phosphorylation in neuronal metabolism. *J Cell Biol* **217**, 2235-2246 (2018). <https://doi.org/10.1083/jcb.201803152>

- 66 Jeon, Y. *et al.* Phenotypic differences between *Drosophila* Alzheimer's disease models expressing human Abeta42 in the developing eye and brain. *Anim Cells Syst (Seoul)* **21**, 160-168 (2017). <https://doi.org/10.1080/19768354.2017.1313777>
- 67 Fernius, J., Starkenberg, A. & Thor, S. Bar-coding neurodegeneration: identifying subcellular effects of human neurodegenerative disease proteins using *Drosophila* leg neurons. *Dis Model Mech* **10**, 1027-1038 (2017). <https://doi.org/10.1242/dmm.029637>
- 68 Iijima-Ando, K. *et al.* Loss of axonal mitochondria promotes tau-mediated neurodegeneration and Alzheimer's disease-related tau phosphorylation via PAR-1. *PLoS Genet* **8**, e1002918 (2012). <https://doi.org/10.1371/journal.pgen.1002918>
- 69 Lin, D. M. & Goodman, C. S. Ectopic and increased expression of Fasciclin II alters motoneuron growth cone guidance. *Neuron* **13**, 507-523 (1994). [https://doi.org/10.1016/0896-6273\(94\)90022-1](https://doi.org/10.1016/0896-6273(94)90022-1)
- 70 Morris, O., Deng, H., Tam, C. & Jasper, H. Warburg-like Metabolic Reprogramming in Aging Intestinal Stem Cells Contributes to Tissue Hyperplasia. *Cell Rep* **33**, 108423 (2020). <https://doi.org/10.1016/j.celrep.2020.108423>
- 71 Tsuyama, T., Tsubouchi, A., Usui, T., Imamura, H. & Uemura, T. Mitochondrial dysfunction induces dendritic loss via eIF2alpha phosphorylation. *J Cell Biol* **216**, 815-834 (2017). <https://doi.org/10.1083/jcb.201604065>
- 72 Geddes, J. F., Hughes, A. J., Lees, A. J. & Daniel, S. E. Pathological overlap in cases of parkinsonism associated with neurofibrillary tangles. A study of recent cases of postencephalitic parkinsonism and comparison with progressive supranuclear palsy and Guamanian parkinsonism-dementia complex. *Brain* **116** (Pt 1), 281-302 (1993). <https://doi.org/10.1093/brain/116.1.281>
- 73 Jenett, A. *et al.* A GAL4-driver line resource for *Drosophila* neurobiology. *Cell Rep* **2**, 991-1001 (2012). <https://doi.org/10.1016/j.celrep.2012.09.011>